

DEEP CONVOLUTIONAL NEURAL NETWORKS IN THE FACE OF CARICATURE: IDENTITY AND IMAGE REVEALED

PREPRINT, COMPILED DECEMBER 31, 2018

Matthew Q. Hill^{1*}, Connor J. Parde¹, Carlos D. Castillo², Y. Ivette Colon¹, Rajeev Ranjan², Jun-Cheng Chen², Volker Blanz³, and Alice J. O’Toole¹

¹The University of Texas at Dallas, U.S.A.

²University of Maryland, U.S.A.

³University of Siegen, Germany

ABSTRACT

Real-world face recognition requires an ability to perceive the unique features of an individual face across multiple, variable images. The primate visual system solves the problem of image invariance using cascades of neurons that convert images of faces into categorical representations of facial identity. Deep convolutional neural networks (DCNNs) also create generalizable face representations, but with cascades of simulated neurons. DCNN representations can be examined in a multidimensional “face space”, with identities and image parameters quantified via their projections onto the axes that define the space. We examined the organization of viewpoint, illumination, gender, and identity in this space. We show that the network creates a highly organized, hierarchically nested, face similarity structure in which information about face identity and imaging characteristics coexist. Natural image variation is accommodated in this hierarchy, with face identity nested under gender, illumination nested under identity, and viewpoint nested under illumination. To examine identity, we caricatured faces and found that network identification accuracy increased with caricature level, and—mimicking human perception—a caricatured distortion of a face “resembled” its veridical counterpart. Caricatures improved performance by moving the identity away from other identities in the face space and minimizing the effects of illumination and viewpoint. Deep networks produce face representations that solve long-standing computational problems in generalized face recognition. They also provide a unitary theoretical framework for reconciling decades of behavioral and neural results that emphasized either the image or the object/face in representations, without understanding how a neural code could seamlessly accommodate both.

Keywords face identification | machine learning technology | primate visual system | illumination | 3D face morphing

People recognize familiar faces effortlessly across changes in viewpoint, illumination, facial expression, and appearance (e.g., glasses, facial hair). The nature of the visual representation that supports this skill is unknown, despite decades of research in psychology and neuroscience [1, 2, 3, 4, 5]. Hypotheses about face representations posit alternatively that the primate visual system reconstructs an object-centered facsimile of a face [1, 6] or that it represents multiple image-based views of faces [4, 3, 7]. The former is consistent with the ability of humans to recognize familiar faces (e.g., friends, family) across a wide range of image and appearance variation. The latter is consistent with well-established difficulties humans have in perceiving “identity constancy” for unfamiliar faces across variable images [8]. Although object-centered and image-based models have made progress on the problem of generalized face/object recognition, neither provides a unified account of how the visual system simultaneously discriminates facial identities while managing (filtering out or encoding) image and appearance variation.

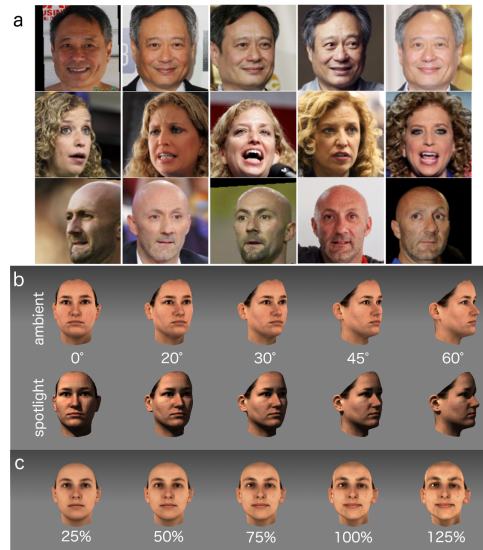


Figure 1: Example of face images used to train and probe the organization of imaging characteristics and subject information in the network. Training was done on real-world unconstrained face images (a). Testing was done on highly controlled laser-scan data varying by viewpoint (b, columns), illumination (b, rows), and identity strength (c).

Author contributions: all authors were involved in conceptualization and design of the methodology of the study. MQH, CJP, CDC, RR, and JC handled software. The original draft was prepared by MQH and AJO. Review and editing were done by MQH, CJP, CDC, YIC, VB, and AJO. Formal analysis, investigation, and visualization were done by MQH and CJP, with validation by MQH, CJP, and CDC. Supervision and funding acquisition were handled by CDC and AJO, with project administration by AJO

University of Maryland has filed a US patent application that covers portions of Network A. RR and CDC are co-inventors on this patent.

*correspondence: matthew.hill@utdallas.edu

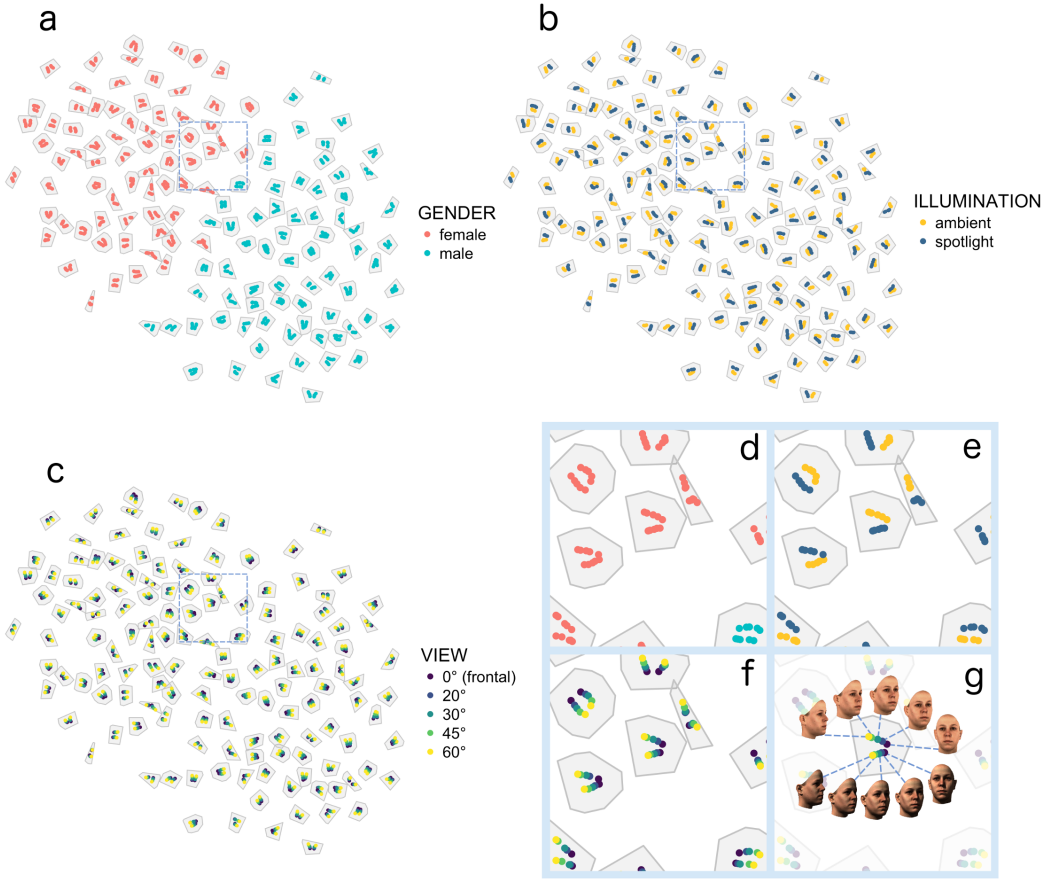


Figure 2: Visualization of top-level DCNN similarity space for all images. The network separates identities accurately (gray polygonal borders surround all images of each identity). The space is divided into male and female sections (a, d). Illumination conditions subdivide within identity groupings (b,e). Viewpoint varies sequentially within illumination clusters (c, f). Dotted-line boxes (a–c) show area covered by zoomed-in sections (d–g).

Computational models, developed in parallel to the psychological and neural theories, illustrate clearly the benefits and pitfalls of object-centered and image-based face representations. In early image-based models, principal components analysis (PCA) was applied to sets of face images [9] to create a *face space* [10]. This model accounts for behavioral findings of a recognition cost for unfamiliar faces when imaging conditions change between learning and test [11]. It also provides insight into the gender [12], race [13], features [14], and identity [12, 15] information in face images. However, image-based PCA works only when the learned and test images are taken under similar conditions (e.g., viewpoint). Thus, it fails to account for the robust nature of human recognition of familiar faces.

The failings of image-based models led to the development of 3D morphable models [16], which represent *faces* rather than *images of faces*. These models operate on densely sampled shape and pigmentation information from laser scans of faces. As with the image-based models, a face space is created by applying PCA to sets of faces. In this space, individual identities are defined as trajectories that radiate out from the average face. As a face moves away from the average along its *identity trajectory*, it becomes increasingly distinctive, changing from anti-caricature

to veridical, and then to caricature. The paradox of caricatures is that they portray a good likeness of a person with a distorted image. Morphable models implement a prototype theory of face recognition [10] and account for caricature perception [17]. They fail as a model of human recognition, because there is no mechanism for a face representation to improve as the face becomes familiar through exposure to more (and more diverse) images [18, 19, 20].

Deep convolutional neural networks are now the state-of-the-art in machine-based face recognition, because they can generalize identity across variable images [21, 22, 23, 24, 25, 26]. These networks are modeled after the primate visual system [27, 28] and consist of multiple layers of simulated neurons that perform nonlinear convolution and pooling operations. DCNN representations expand in early layers of the network, but are compressed in the top layers through a bottle-neck of neurons. The representation of facial identity that emerges at the final layer of a DCNN is compact and can operate robustly over changes in image parameters (e.g., viewpoint) and appearance.

DCNN face representations have characteristics of both object-centered and image-based codes. Similar to object-centered models, they represent identity with an image-invariant code.

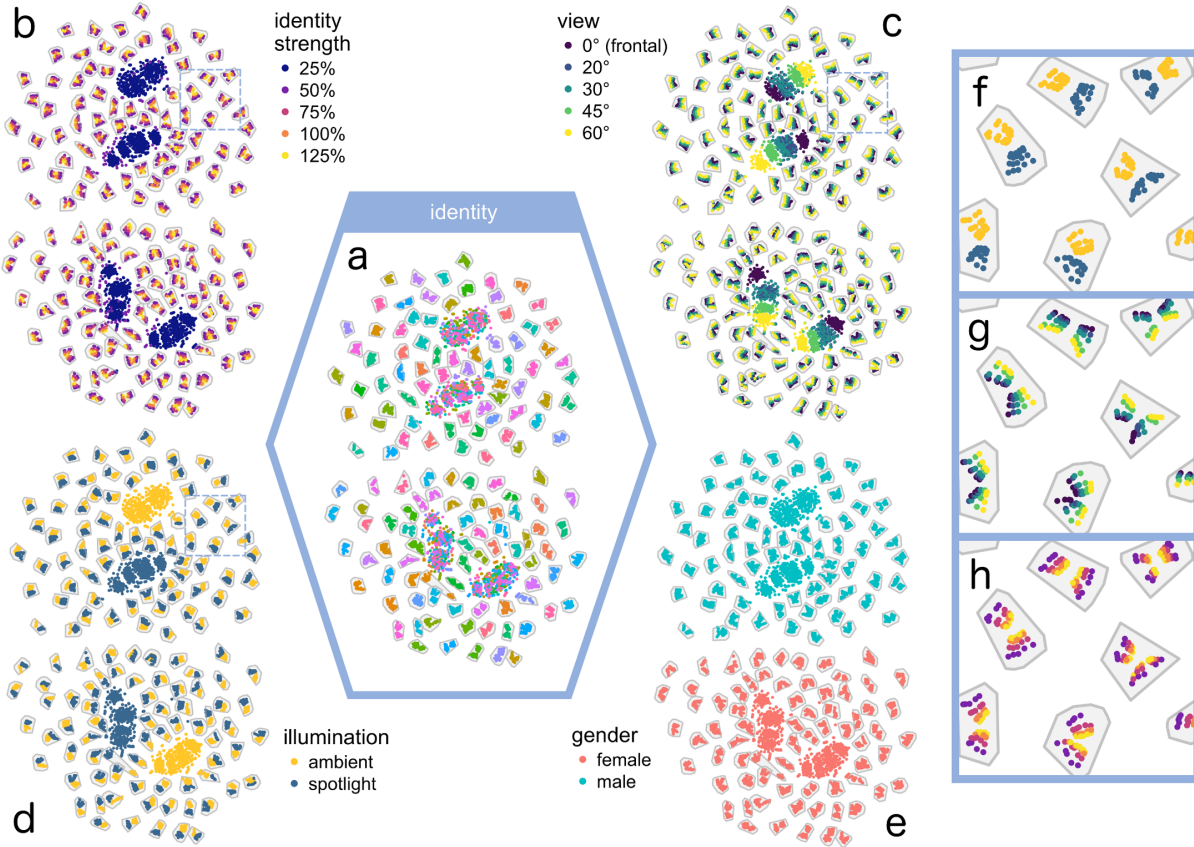


Figure 3: Visualization of top-level similarity space with identity strength variation. Mixed-identity clusters appear in addition to identity-constant clusters (a), with these mixed regions containing weak identity strength images (b). Each identity-mixed cluster contains images of a single viewpoint (c), nested within a single illumination condition (d), within a gender group (e). Zoomed-in sections (f–h) show that, within an identity cluster, images divide by illumination conditions (f); viewpoints divide with caricature levels arranged in string-shapes (g); caricatures fall in the center of the identity cluster (h). Gray polygons contain all images of an identity where identity strength is $\geq 75\%$.

Similar to image-based models, DCNN representations retain information about the images they process [29, 30]. Specifically, features from the top-layer of DCNNs trained for face recognition support reliable linear read-out of the viewpoint (yaw in degrees, pitch as on-center versus up/down) of the input image [29].

Deep networks offer a proof-of-principle that a robust and general coding of high level visual information can co-exist with instance-based codes that retain characteristics of the imaging conditions. But how do DCNN codes accomplish the balancing act of accommodating facial identity and image information in a unitary representation? It has been difficult to directly address this question because viewpoint, illumination, and the number/quality of images for each identity are not controlled in datasets typically used to train DCNNs. To overcome this challenge, we probed a network trained with “in-the-wild” face images using an “in-the-lab” dataset. Specifically, we used highly controlled laser scans of faces to examine how DCNNs represent faces in terms of their subject parameters (identity and gender) and image characteristics (viewpoint and illumination). To probe the nature of the identity representation in these

networks, we manipulated the strength of identity information in a face with caricatures. The results show that DCNNs produce a remarkably organized representation of faces that is consistent with human perception of face identity across variable images and across caricature “distortions”.

Results

Face Space Visualization

We examined the organization of imaging characteristics and subject variables in the DCNN top-layer face representation using a *face space* framework [10, 31]. In this framework, the distance between points in the space reflects the similarity of face images as “perceived” by the top layer of the DCNN. We report data on a 101-layered face identification DCNN [26] trained with 5,714,444 in-the-wild images (see Fig. 1A) of 58,020 identities. The top-layer output of the network is a 512-element face representation. Images were created from laser-scans of 70 male and 70 female heads registered to a parametric 3D face model [16]. Each face was rendered from five viewpoints (yaw: 0° [frontal], 20°, 30°, 45°, 60° [left profile]) under two

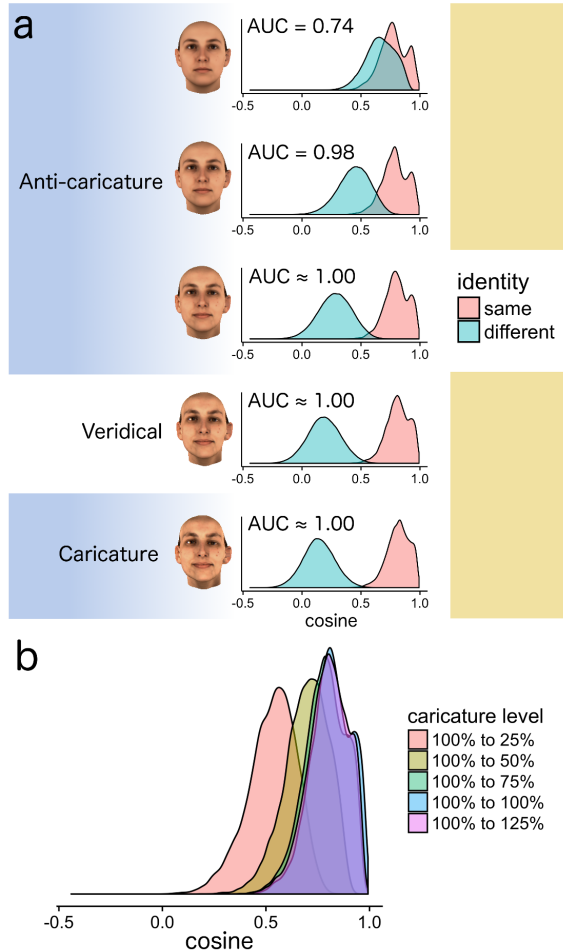


Figure 4: (a) Image-pair similarity score distributions show that accuracy increases with caricature level. This is due to the greater dissimilarity of caricatures to other identities (leftward drift of the different-identity distribution). (b) Similarity distributions across caricature levels show that the veridical is similar to the caricature and the 75% anti-caricature, but not to weak anti-caricatures ($\leq 50\%$).

illumination conditions (ambient, directional spotlight). This produced 1,400 images (Fig. 1B), which we processed through the DCNN to produce a top-layer representation for each image. To examine the structure and information content of the face space that emerges at the top layer of units in DCNNs, we visualized the face-space representations of the 1,400 images using *t*-distributed Stochastic Neighbor Embedding (*t*-SNE) [32, 33].

Figure 2 shows the hierarchical organization of the face space with respect to gender, identity, illumination, and viewpoint. Identities were separated with high accuracy (Area Under the Curve [AUC] ≈ 1), indicating that the DCNN recognizes faces across substantial variability in viewpoint and illumination. The space is separated roughly into two clusters by gender (Fig. 2A). Within each identity cluster, face images from the two illumination conditions separate into sub-clusters (Fig. 2B, E). Within each illumination sub-cluster, images are arranged

systematically by viewpoint, like beads on a chain (Fig. 2C, F). This demonstrates a highly organized representation of image information in a robust identity code.

Next, we quantified the accessibility of gender, illumination, and viewpoint in the full high-dimensional space, using a linear classifier. All three variables were predicted accurately from the face representations ($p < .001$, in all cases). Viewpoint was detected with an average error of 6.34° ($SD = 4.95^\circ$), illumination classification was 95.21% correct, and gender classification was 98.21% correct. This demonstrates accurate linear read-out of image and subject information from the top-layer face representation.

Identity Strength in the Face Space

To examine facial distinctiveness, we used the 3D head model to generate morphs that varied in the strength of the identity information in the face [31]. Following the identity trajectory, each face was morphed from a caricature (high identity strength) to a near-average face (low identity strength) in four equal steps. This yielded five versions of each face (125% [caricature]; 100% [veridical]; 75%, 50%, 25% [anti-caricature]). The addition of identity strength increased the dataset to 7,000 images (Fig. 1C).

Figure 3 shows the *t*-SNE face space with the inclusion of identity strength variation. It shows that faces with weak identity information are grouped according to other variables (gender, view, illumination). Specifically, Fig. 3A shows that mixed-identity clusters are scattered among correctly clustered identities, and Fig. 3B shows that mixed-identity regions contain only faces with weak identity strength. Each identity-mixed cluster contains images of a single viewpoint (Fig. 3C), nested within a single illumination condition (Fig. 3D), and within a gender group (Fig. 3E). Zoomed-in sections (F–H) show that within an identity cluster, images divide by illumination conditions (Fig. 3F). Viewpoints also divide, with caricature levels arranged in string-like groups (Fig. 3G). Caricatures are centered in identity clusters (Fig. 3H), showing that same-identity caricatures cluster more closely over image variation than veridicals and anti-caricatures (see also SI).

Caricature and Identity

Face identification amounts to a decision of whether two images depict the same or different identities. This decision is based on the cosine similarity between the top-layer representations of the two images (higher similarities suggest the same identity). Accuracy can be visualized using the similarity distributions for same- and different-identity image pairs (wider separation indicates higher accuracy).

Figure 4A shows that caricaturing improves the network’s identification accuracy by increasing the “perceptual” contrast between faces as caricature level increases (leftward drift of different-identity distribution). Caricaturing does not appreciably move the same-identity distribution. However, consistent with its effects on minimizing the impact of imaging parameters (Fig. 3H), the range of similarity values in this distribution compresses as caricature level increases (see SI). Next, we asked whether the DCNN “sees” the caricature as the same identity as its corresponding veridical face. Figure 4B indicates that it does. We looked at the similarity between veridicals

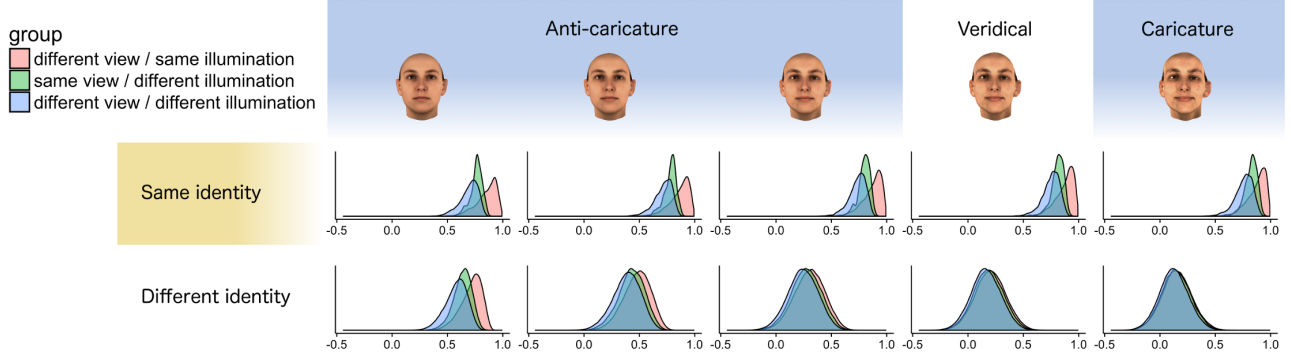


Figure 5: Density curves of face image-pair cosine similarity scores. Overlap between same-identity (top row) and different-identity (bottom row) distributions decreases as identity strength increases. Within same-identity distributions, viewpoint and illumination differences are visible at all caricature levels as peaks in the distributions. These peaks are visible in the different-identity distributions only for weak identity strengths.

and their corresponding images across caricature level. The network perceives 75% anti-caricatures and caricatures as nearly equivalent to veridicals (Fig. 4B). The 25% and 50% anti-caricatures are less similar to their veridical faces.

Caricaturing, therefore, affects DCNN perception by exaggerating a face’s unique identity information relative to other faces in the population without impairing identity perception.

Caricature and Image Conditions: Viewpoint and Illumination

How does image-based information interact with identity constancy? Figure 5 shows that imaging conditions affect the DCNN’s perception of face similarity. Changes in viewpoint and/or illumination can be seen as peaks in the similarity score distributions for same-identity pairs (top row), at all levels of caricature. For higher identity strengths ($\geq 75\%$), different-identity distributions (bottom-row) separate visibly from same-identity distributions, and the salience of image-based similarity is attenuated. This shows that identity—not imaging condition—is the primary determiner of dissimilarity for different-identity pairs. Imaging condition effects reappear with weak identity strengths ($\leq 50\%$). These near-average faces approach a single (average) identity that varies only by imaging condition. Therefore, similarity in the DCNN encompasses both identity and viewing conditions, but on a different scale. Identity contributes far more than image conditions.

Discussion

Deep networks accomplish the balancing act of accommodating facial identity and image information in a unitary representation by generating an elegantly organized face similarity space. To understand this organization, it is useful to distinguish between person properties (e.g., identity, gender, race) and specific image encounters (e.g., viewpoint, illumination). The former, immutable characteristics, divide the face space into subspace partitions that are homogeneous with respect to their defining person characteristics. The latter, variable properties, are accommodated within the homogeneous subspaces, yet they apply to all identities.

Being able to access information about object/person properties at multiple levels of abstraction is a computational goal of a visual categorization system [34]. In psychological terms, the topology of the DCNN space organizes faces to allow easy access to person properties at different levels of abstraction. The space itself defines a basic-level category of faces. The position of an image in the face space indicates a subordinate gender-category, and the position in this gender category specifies an exemplar category of identity [35, 34].

To access the fundamental person property of identity, the DCNN must code the uniqueness of a face across variable image conditions. The robust nature of this unique identity information in a DCNN is inherited from the topology of its similarity space, which is highly non-linear with respect to image properties. Two widely different images (e.g, frontal versus profile) are coded as similar, because the network represents identity categorically. The use of caricaturing to probe the organization of the face space provides a unique vantage point for seeing how identity and image information interact in a DCNN. Caricaturing affects the DCNN performance because it operates both within individual identity clusters and at the level of face populations. Within identity clusters, caricatured faces minimize the influence of imaging parameters. At the population level, caricaturing increases the separation between face identities in the space, making them all less confusable.

From a psychological perspective, the DCNN’s combined representation of identity and image encounters provides a unified account of behavioral effects seen previously as evidence for exclusively image-based *or* object-centered theories of face processing. DCNN representations are compatible with a face recognition cost for changes in image parameters between learning and testing. They are also compatible with effects of face distinctiveness relative to a population. The general accord between behavioral results and deep network representations, combined with the network’s ability to produce a robust representation of identity, makes DCNNs a plausible model of human face processing. The present work with in-the-lab images points to the possibility of addressing how “familiarity” with a face, via exposure to in-the-wild images, might alter the capacity of the face representation to generalize recognition even

further. There are multiple stages of DCNN training that can be targeted in this endeavor [30].

From a neuroscience perspective, DCNN representations reconcile the seemingly paradoxical nature of ventral temporal cortex organization as both object-categorical *and* reflective of low level image properties, e.g., viewpoint [36, 37], illumination [38], size [39], and position [40]. For the former, structure exists in the organization of person properties in subspaces. For the latter, structure within identity subspaces is duplicated across identities to index image properties.

From a computational perspective, converting a representation in the image domain to one that operates in a categorical domain, does not necessarily entail information loss. Instead it can be achieved by reorganizing the space. Although much of what we see of this organization here is sufficiently salient to be visualized in two dimensions, the full representation in the high dimensional space drives these effects (and our computations). If the goal of a visual system is to reorganize the representational codes to “untangle” information that is non-linear in the image domain [41], then the data configurations we arrive at here may offer a first look at how cascades of neural-like computations can represent face identity robustly with limited loss of image context.

Methods

Networks

To test the stability of the face space across network architectures and training data, we performed these simulations on two face identification DCNNs: Network A [42, 43] (main text), and Network B [44]. Network A is a ResNet-based DCNN trained with the Universe dataset [42, 43], which is a mixture of three datasets (UMDFaces [45], UMDVideos [42], and MS1M [46]). It includes images and video frames acquired in extremely challenging, in-the-wild conditions (pose, illumination, etc.). We used the ResNet-101 [47] architecture with the Crystal Loss (L2 Softmax) loss function for training [43]. ResNet-101 consists of 101 layers organized with skip connections that retain error signal strength to leverage very deep CNN architectures. Scale factor α was set to 50. The final layer of the fully-trained network was removed and the penultimate layer (512 features) was used as the identity descriptor. Once the training is complete, this penultimate layer is considered the “top layer.” Network B has 15 convolution and pooling layers, a dropout layer, and a fully connected top layer that outputs a 320-dimensional identity descriptor. Network B was trained using a softmax loss function on the CASIA-WebFace dataset (494,414 images of 10,575 identities that vary widely in illumination, viewpoint, and overall quality [blur, facial occlusion, etc.]).

Morphing Stimuli

Stimuli were made from 3D laser scans with densely sampled shape and reflectance data from faces. These scans were put into point-by-point correspondence with an average face. In this format, a face is described as a deformation field from the average face, in shape $[\delta x, \delta y, \delta z]$ and reflectance $[\delta r, \delta g, \delta b]$. Identity strength was manipulated by multiplying the face representation by a scalar value, s , such that $s > 1$ produces a caricature; and $0 < s < 1$ produces an anti-caricature.

Visualization

Face space visualizations were done with *t*-SNE, a non-linear dimensionality reduction technique that uses gradient descent to preserve the distance between each point in a high-dimensional space, while reducing the number of dimensions [32]. DCNNs use the angular distance between representations to compare images. To preserve this relationship in the space, face representation vectors were normalized to unit length before computing the *t*-SNE. We used the Barnes-Hut implementation of *t*-SNE [33] with a θ of 0.5, and perplexity coefficients of 30 (Fig. 2) and 100 (Fig. 3). *t*-SNE was used to reduce the DCNN’s 512-dimensional feature space to a two-dimensional space. However, all quantitative analyses were conducted in the full 512-dimensional space.

Classification

Linear discriminant analysis (LDA) was applied to the full-dimensional face descriptors to classify gender and illumination. Linear regression with the Moore-Penrose pseudo-inverse was used to predict viewpoint. Predictions were conducted with identity-level cross-validation. Classifications generated from Network B produced results similar to those generated from Network A (see SI). Statistical significance of the Network A predictions were evaluated with permutation tests. A null distribution was generated from the original data matrix by creating random permutations of the column contents. Permutations ($n = 1000$) were generated for each variable (gender, illumination, viewpoint). Resulting distributions were compared to the true value from each classification test. All permutation tests proved significant at $p < .001$, with no overlap between test value and null distribution. Network B produced the same results.

Acknowledgements

Funding: Supported by the Intelligence Advanced Research Projects Activity (IARPA). This research is based upon work supported by the Office of the Director of National Intelligence (ODNI), Intelligence Advanced Research Projects Activity (IARPA), via IARPA R&D Contract No. 2014-14071600012. The views and conclusions contained herein are those of the authors and should not be interpreted as necessarily representing the official policies or endorsements, either expressed or implied, of the ODNI, IARPA, or the U.S. Government. The U.S. Government is authorized to reproduce and distribute reprints for Governmental purposes notwithstanding any copyright annotation thereon.

References

- [1] David Marr. Vision: A computational investigation into the human representation and processing of visual information. mit press. *Cambridge, Massachusetts*, 1982.
- [2] Roberto Brunelli and Tomaso Poggio. Face recognition: Features versus templates. *IEEE transactions on pattern analysis and machine intelligence*, 15(10):1042–1052, 1993.
- [3] Maximilian Riesenhuber and Tomaso Poggio. Hierarchical models of object recognition in cortex. *Nature neuroscience*, 2(11):1019, 1999.
- [4] Heinrich H Bülthoff and Shimon Edelman. Psychophysical support for a two-dimensional view interpolation theory of object recognition. *Proceedings of the National Academy of Sciences*, 89(1):60–64, 1992.

- [5] Alan L Yuille. Deformable templates for face recognition. *Journal of Cognitive Neuroscience*, 3(1):59–70, 1991.
- [6] Irving Biederman. Recognition-by-components: a theory of human image understanding. *Psychological review*, 94(2):115, 1987.
- [7] T. Poggio and S. Edelman. A network that learns to recognize three-dimensional objects. *Nature*, 343(6255):263–266, 1990. ISSN 0028-0836. doi: 10.1038/343263a0. URL <http://www.nature.com/doifinder/10.1038/343263a0>.
- [8] Rob Jenkins, David White, Xandra Van Montfort, and A Mike Burton. Variability in photos of the same face. *Cognition*, 121(3):313–323, 2011.
- [9] Matthew Turk and Alex Pentland. Eigenfaces for recognition. *Journal of cognitive neuroscience*, 3(1):71–86, 1991.
- [10] Tim Valentine. A unified account of the effects of distinctiveness, inversion, and race in face recognition. *The Quarterly Journal of Experimental Psychology Section A*, 43(2):161–204, 1991.
- [11] Nikolaus F Troje and Heinrich H Bülthoff. Face recognition under varying poses: The role of texture and shape. *Vision research*, 36(12):1761–1772, 1996.
- [12] Alice J O’Toole, Hervé Abdi, Kenneth A Deffenbacher, and Dominique Valentin. Low-dimensional representation of faces in higher dimensions of the face space. *JOSA A*, 10(3):405–411, 1993.
- [13] Alice J O’Toole, Kenneth A Deffenbacher, Dominique Valentin, and Herve Abdi. Structural aspects of face recognition and the other-race effect. *Memory & Cognition*, 22(2):208–224, 1994.
- [14] Adrian Nestor, David C Plaut, and Marlène Behrmann. Feature-based face representations and image reconstruction from behavioral and neural data. *Proceedings of the National Academy of Sciences*, 113(2):416–421, 2016.
- [15] Alice J O’Toole, Richard B Millward, and James A Anderson. A physical system approach to recognition memory for spatially transformed faces. *Neural Networks*, 1(3):179–199, 1988.
- [16] Volker Blanz and Thomas Vetter. A morphable model for the synthesis of 3d faces. In *Proceedings of the 26th annual conference on Computer graphics and interactive techniques*, pages 187–194. ACM Press/Addison-Wesley Publishing Co., 1999.
- [17] Gillian Rhodes, Susan Brennan, and Susan Carey. Identification and ratings of caricatures: Implications for mental representations of faces. *Cognitive Psychology*, 19(4):473–497, 1987. ISSN 00100285. doi: 10.1016/0010-0285(87)90016-8.
- [18] Jacqueline G. Cavazos, Eilidh Noyes, and Alice J. O’Toole. Learning context and the other-race effect: Strategies for improving face recognition, 2018. ISSN 18785646.
- [19] A. J. Dowsett, A. Sandford, and A. Mike Burton. Face learning with multiple images leads to fast acquisition of familiarity for specific individuals. *Quarterly Journal of Experimental Psychology*, 69(1):1–10, 2016. ISSN 17470226. doi: 10.1080/17470218.2015.1017513.
- [20] Kay L. Ritchie and A. Mike Burton. Learning faces from variability. *Quarterly Journal of Experimental Psychology*, 70(5):897–905, 2017. ISSN 17470226. doi: 10.1080/17470218.2015.1136656.
- [21] Yi Sun, Xiaogang Wang, and Xiaoou Tang. Deep learning face representation from predicting 10,000 classes. In *Proceedings of the IEEE conference on computer vision and pattern recognition*, pages 1891–1898, 2014.
- [22] Yaniv Taigman, Ming Yang, Marc’Aurelio Ranzato, and Lior Wolf. Deepface: Closing the gap to human-level performance in face verification. In *Proceedings of the IEEE conference on computer vision and pattern recognition*, pages 1701–1708, 2014.
- [23] Swami Sankaranarayanan, Azadeh Alavi, Carlos Castillo, and Rama Chellappa. Triplet probabilistic embedding for face verification and clustering. *arXiv preprint arXiv:1604.05417*, 2016.
- [24] Florian Schroff, Dmitry Kalenichenko, and James Philbin. Facenet: A unified embedding for face recognition and clustering. In *Proceedings of the IEEE conference on computer vision and pattern recognition*, pages 815–823, 2015.
- [25] Jun-Cheng Chen, Rajeev Ranjan, Amit Kumar, Ching-Hui Chen, Vishal M Patel, and Rama Chellappa. An end-to-end system for unconstrained face verification with deep convolutional neural networks. In *Proceedings of the IEEE International Conference on Computer Vision Workshops*, pages 118–126, 2015.
- [26] Rajeev Ranjan, Swami Sankaranarayanan, Carlos D Castillo, and Rama Chellappa. An all-in-one convolutional neural network for face analysis. In *Automatic Face & Gesture Recognition (FG 2017), 2017 12th IEEE International Conference on*, pages 17–24. IEEE, 2017.
- [27] Kunihiko Fukushima. Neocognitron: A hierarchical neural network capable of visual pattern recognition. *Neural networks*, 1(2):119–130, 1988.
- [28] Alex Krizhevsky, Ilya Sutskever, and Geoffrey E Hinton. Imagenet classification with deep convolutional neural networks. In *Advances in neural information processing systems*, pages 1097–1105, 2012.
- [29] Connor J Parde, Carlos Castillo, Matthew Q Hill, Y Ivette Colon, Swami Sankaranarayanan, Jun-Cheng Chen, and Alice J O’Toole. Face and image representation in deep cnn features. In *Automatic Face & Gesture Recognition (FG 2017), 2017 12th IEEE International Conference on*, pages 673–680. IEEE, 2017.
- [30] Alice J O’Toole, Carlos D Castillo, Connor J Parde, Matthew Q Hill, and Rama Chellappa. Face Space Representations in Deep Convolutional Neural Networks. *Trends in cognitive sciences*, 2018.
- [31] David A Leopold, Alice J O’Toole, Thomas Vetter, and Volker Blanz. Prototype-referenced shape encoding revealed by high-level aftereffects. *Nature neuroscience*, 4(1):89, 2001.
- [32] Laurens van der Maaten and Geoffrey Hinton. Visualizing data using t-sne. *Journal of machine learning research*, 9(Nov):2579–2605, 2008.

- [33] Laurens Van Der Maaten. Accelerating t-sne using tree-based algorithms. *The Journal of Machine Learning Research*, 15(1):3221–3245, 2014.
- [34] Kalanit Grill-Spector and Kevin S Weiner. The functional architecture of the ventral temporal cortex and its role in categorization. *Nature Reviews Neuroscience*, 15(8):536, 2014.
- [35] Eleanor Rosch, Carolyn B Mervis, Wayne D Gray, David M Johnson, and Penny Boyes-Braem. Basic objects in natural categories. *Cognitive psychology*, 8(3):382–439, 1976.
- [36] Tim C Kietzmann, Sonia Poltoratski, Peter König, Randolph Blake, Frank Tong, and Sam Ling. The occipital face area is causally involved in facial viewpoint perception. *Journal of Neuroscience*, 35(50):16398–16403, 2015.
- [37] Vaidehi S Natu, Fang Jiang, Abhijit Narvekar, Shaiyan Keshvari, Volker Blanz, and Alice J O’Toole. Dissociable neural patterns of facial identity across changes in viewpoint. *Journal of Cognitive Neuroscience*, 22(7):1570–1582, 2010.
- [38] Kalanit Grill-Spector, Tammar Kushnir, Shimon Edelman, Galia Avidan, Yacov Itzhak, and Rafael Malach. Differential processing of objects under various viewing conditions in the human lateral occipital complex. *Neuron*, 24(1):187–203, 1999.
- [39] Xiaomin Yue, Brittany S Cassidy, Kathryn J Devaney, Daphne J Holt, and Roger BH Tootell. Lower-level stimulus features strongly influence responses in the fusiform face area. *Cerebral Cortex*, 21(1):35–47, 2010.
- [40] Kendrick N Kay, Kevin S Weiner, and Kalanit Grill-Spector. Attention reduces spatial uncertainty in human ventral temporal cortex. *Current Biology*, 25(5):595–600, 2015.
- [41] James J DiCarlo and David D Cox. Untangling invariant object recognition. *Trends in cognitive sciences*, 11(8):333–341, 2007.
- [42] Ankan Bansal, Carlos D Castillo, Rajeev Ranjan, and Rama Chellappa. The do’s and don’ts for cnn-based face verification. In *ICCV Workshops*, pages 2545–2554, 2017.
- [43] Rajeev Ranjan, Ankan Bansal, Hongyu Xu, Swami Sankaranarayanan, Jun-Cheng Chen, Carlos D Castillo, and Rama Chellappa. Crystal loss and quality pooling for unconstrained face verification and recognition. *arXiv preprint arXiv:1804.01159*, 2018.
- [44] Jun-Cheng Chen, Vishal M Patel, and Rama Chellappa. Unconstrained face verification using deep cnn features. In *Applications of Computer Vision (WACV), 2016 IEEE Winter Conference on*, pages 1–9. IEEE, 2016.
- [45] Ankan Bansal, Anirudh Nanduri, Carlos D Castillo, Rajeev Ranjan, and Rama Chellappa. Umdfaces: An annotated face dataset for training deep networks. In *Biometrics (IJCB), 2017 IEEE International Joint Conference on*, pages 464–473. IEEE, 2017.
- [46] Yandong Guo, Lei Zhang, Yuxiao Hu, Xiaodong He, and Jianfeng Gao. Ms-celeb-1m: A dataset and benchmark for large-scale face recognition. In *European Conference on Computer Vision*, pages 87–102. Springer, 2016.
- [47] Yandong Wen, Kaipeng Zhang, Zhifeng Li, and Yu Qiao. A discriminative feature learning approach for deep face recognition. In *European Conference on Computer Vision*, pages 499–515. Springer, 2016.

Supplemental Information

In this supplemental information section we report further details and additional analyses for Network A. We also report replications using Network B for classification analysis and network performance.

Face Space Visualization

Classification Replication

Linear discriminant analysis (LDA) was applied to the full-dimensional face descriptors to classify gender and illumination. Linear regression with the Moore-Penrose pseudo-inverse was used to predict viewpoint. Predictions were conducted with identity-level cross-validation. Classifications generated from Network B produced results similar to those generated from Network A.

Table 1: Classification and regression results for Networks A and B. Percentages (%) denote classification percent correct, while degrees ($^{\circ}$) denote average prediction error.

	Gender	Illumination	Viewpoint (SD)
Network A	98.21%	95.21%	6.34 $^{\circ}$ (4.95 $^{\circ}$)
Network B	90.98%	97.44%	7.28 $^{\circ}$ (5.73 $^{\circ}$)

Permutation

Statistical significance of Network A predictions were evaluated with permutation tests. A null distribution was generated from the original data matrix by creating random permutations of the column contents. Permutations ($n = 1000$) were generated for each variable (gender, illumination, viewpoint). Resulting distributions were compared to the true value from each classification test. All permutation tests proved significant at $p < .001$, with no overlap between test value and null distribution.

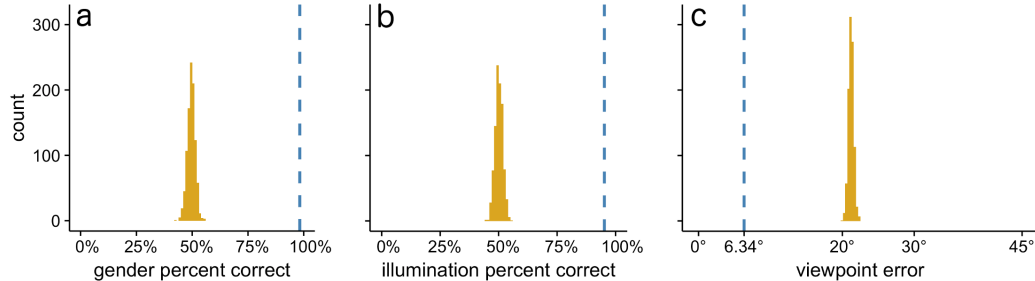


Figure S1: Permutation results for Network A show the statistical significance of regression and classification analyses. Yellow histograms show null distributions comprised of 1,000 permutations. Blue dotted lines show test values. Gender showed no overlap between null and test value 98.21 (a), illumination showed no overlap between null and test value 95.21 (b), viewpoint showed no overlap between null and test value 6.34 (c).

Caricature and Identity

Network Performance

We measured the network's identification performance using area under the ROC curve (AUC). It is common in much of the face recognition literature on computational models to construct the distribution of different-identity image pairs from all possible pairs of images of different identities. Strictly speaking, however, to measure face identification performance, it is more conservative to control for factors other than identity (e.g., gender) that could underlie dissimilarity between faces. Therefore, the AUCs reported in Figure 4A (main text) include only same-gender image pairs in the different-identity distribution.

Comparable data to those reported in Figure 4A for Network B are displayed in Table S2.

Table 2: AUC scores of each DCNN at each identity strength level.

Identity Strength	25%	50%	75%	100%	125%
Network A (AUC)	0.735	0.979	0.999	1.000	1.000
Network B (AUC)	0.673	0.911	0.983	0.996	0.998

Identity Constancy and Caricature

Figure S2 shows that the similarity scores for same-identity pairs increase marginally with caricature level. This demonstrates a small graded improvement in identity constancy over changes in view and illumination as identity strength increases.

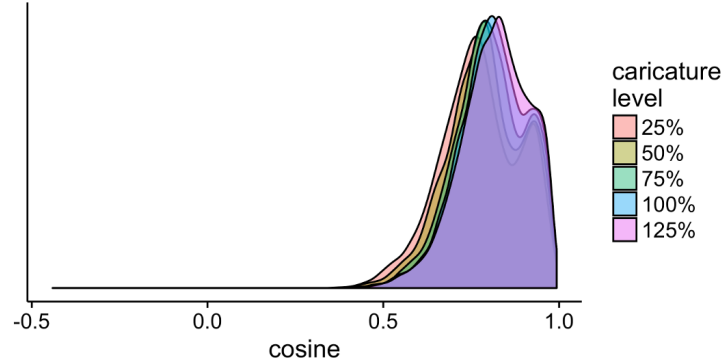


Figure S2: Distributions of same-identity similarity scores show that identity constancy increases with caricature level. As the caricature level increases, the range of similarity values from matched-identity image comparisons compresses towards 1.

Imaging Conditions and Caricature

Figure S3 shows a complete breakdown of the effects of viewpoint and illumination on similarity scores for same- and different-identity image pairs across caricature levels. This complements Figure 4A in the main text that shows the complete dataset without dividing by the type (viewpoint, illumination, illumination and viewpoint) of image mismatch.

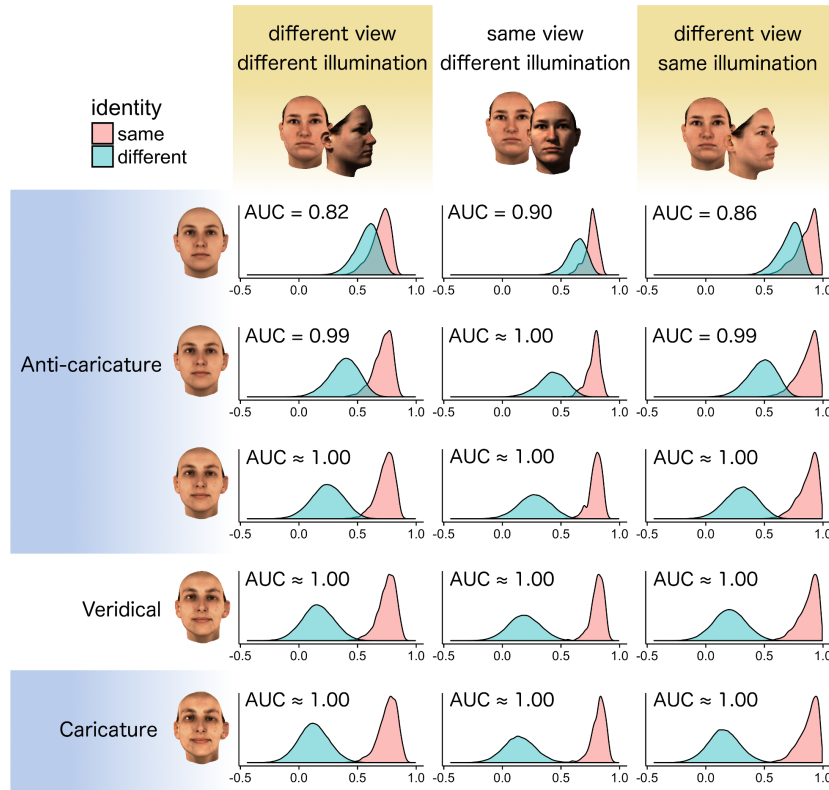


Figure S3: Image-pair similarity distributions show that identification accuracy increases with caricature level. This effect is consistent across image comparisons including changes in both viewpoint and illumination, changes in only illumination, and changes in only viewpoint. This increase in identification accuracy is the result of a leftward drift of the non-match distribution and demonstrates that caricaturing benefits performance by accentuating the image features that make two different identities look less like one another.